Relation of extended Van Hove singularities to high-temperature superconductivity within strong-coupling theory

R. J. Radtke*
Department of Physics and The James Franck Institute, The University of Chicago, Chicago, Illinois 60637

M. R. Norman
Materials Science Division, Argonne National Laboratory, Argonne, Illinois 60439
(Received 22 April 1994)

Recent angle-resolved photoemission (ARPES) experiments have indicated that the electronic dispersion in some of the cuprates possesses an extended saddle point near the Fermi level which gives rise to a density of states that diverges like a power law instead of the weaker logarithmic divergence usually considered. We investigate whether this strong singularity can give rise to high transition temperatures by computing the critical temperature T_c and isotope effect coefficient α within a strong-coupling Eliashberg theory which accounts for the full energy variation of the density of states. Using band structures extracted from ARPES measurements, we demonstrate that, while the weak-coupling solutions suggest a strong influence of the strength of the Van Hove singularity on T_c and α, strong-coupling solutions show less sensitivity to the singularity strength and do not support the hypothesis that band-structure effects alone can account for either the large T_c's or the different T_c's within the copper oxide family. This conclusion is supported when our results are plotted as a function of the physically relevant self-consistent coupling constant, which shows universal behavior at very strong coupling.

On general grounds, we know that low-dimensional features in the electronic dispersion lead to singularities in the density of states, and we also expect that the superconducting critical temperature T_c will be enhanced when the Fermi level lies near one of these singularities. Early work along these lines focused on the A15 superconductors, where the low-dimensional features are one-dimensional chains, and calculations in both BCS (Refs. 1 and 2) and Eliashberg[3–5] formalisms demonstrated a small but significant enhancement of T_c. Current interest is in the family of high-temperature cuprate superconductors, where the low-dimensional structures are the CuO_2 planes. Energy dispersions from photoemission measurements and local density approximation (LDA) band-structure calculations led a number of workers to suggest that the density of states in these compounds was logarithmically divergent and that this divergence, in addition to a fairly typical pairing boson, could account for the large critical temperatures, the anomalous isotope effect, and the specific heat.[6–8] This picture of the origin of high-temperature superconductivity has become known as the "Van Hove scenario." While a logarithmic singularity is appropriate for $La_{2-x}Sr_xCuO_4$ (LSCO), recent photoemission measurements on $YBa_2Cu_3O_{6.9}$ (YBCO), $YBa_2Cu_4O_8$, and $Bi_2Sr_2CaCu_2O_8$ (BSCCO) suggest that the density of states in these materials has a much stronger power law divergence.[9–11] Weak-coupling BCS calculations suggest that the enhancement of T_c due to these power law singularities would be much larger than that for the logarithmic singularity and may account for the larger T_c's observed in these compounds.[10]

One difficulty with relying on singularities in the density of states to produce large critical temperatures is that quasiparticle lifetime effects smear out the singularities and so must be treated carefully to insure correct results. Even before the discovery of the cuprate superconductors, Hirsch and Scalapino carried out such calculations for the logarithmic Van Hove singularities present in a simple two-dimensional tight-binding band with a superconducting pairing provided by an attractive Hubbard interaction.[12] For weak interactions, they found that the effects of quasiparticle lifetime and higher-order corrections to the interaction reduced but did not eliminate the T_c enhancement that occurs when the Van Hove singularity coincides with the Fermi level.[12] For strong interactions, many authors have carried out calculations in connection with the cuprates and find that the critical temperatures are not as strongly enhanced by logarithmic[13,14] or δ-function[15] Van Hove singularities as weak-coupling calculations would suggest and that strong-coupling effects smear out the density of states peak.[16,17]

In this paper, we extend these results by using tight-binding fits to photoemission data on the cuprates as input to a strong-coupling Eliashberg T_c calculation. We address several questions. Does a power law Van Hove singularity significantly enhance T_c over that given by a logarithmic one? How much is T_c enhanced as a function of singularity strength relative to a flat density of states? And, how does the strength of the electron-pairing boson interaction affect our answers to these questions? We find that the dramatic increase in T_c due to the Van Hove singularity in weak-coupling theory is moderated considerably by strong-coupling effects and that the enhancement of T_c by a power law singularity over a logarithmic one is also reduced somewhat by strong-coupling effects. We suggest several possible extensions of this

work, though, which should be investigated before drawing a negative conclusion concerning the Van Hove scenario for the cuprates.

For computing the critical temperatures, we use the standard mean field formalism[18] in which the electron self-energy is solved self-consistently from the single-exchange graph generalized to include the energy dependence of the density of states.[4,5,19] For simplicity, we take the pairing interaction to be an Einstein phonon with frequency $\Omega_0 = 500$ K (43 meV), and we assume that the electron-phonon matrix element g is independent of wave vector. The equations for the electron self-energy in Matsubara space $\Sigma(i\omega_n)$ can then be written in the Nambu matrix notation[18] as

$$\Sigma(i\omega_n) = -T\sum_m g^2 D(i\omega_n - i\omega_m) \times \int dE\, N(E)\,\tau_3 G(E, i\omega_m)\tau_3, \quad (1)$$

where $G(E, i\omega_n)$ is the electron Green's function which satisfies the Dyson equation

$$G^{-1}(E, i\omega_n) = G_0^{-1}(E, i\omega_n) - \Sigma(i\omega_n) \quad (2)$$

with $G_0(E, i\omega_n)$ being the bare propagator. In these expressions, T is the temperature, g^2 is the electron-phonon coupling constant, D is the phonon propagator, $N(E)$ is the single-spin density of states per unit cell, τ_3 is the third Pauli matrix, and $\omega_n = (2n+1)\pi T$ are fermionic Matsubara frequencies. Throughout this paper, we set $\hbar = k_B = 1$. We solve these self-energy equations for all components of the Nambu self-energy (τ_0, τ_1, and τ_3) (Ref. 18) and at fixed band filling n determined by

$$n = 1 + \sum_n e^{-i\omega_n 0+} \int dE\, N(E)\,\mathrm{Tr}\,[\tau_3 G(E, i\omega_n)]. \quad (3)$$

We fix n in order to properly account for the loss of particle-hole symmetry in the interacting system, but we note that, due to the uncertainties in the parametrization of the band structures from ARPES data described below, the absolute values of n should not be taken too seriously. Note that this approach includes the effects of inelastic pair breaking, which is important for obtaining reasonable T_c estimates. We linearize these equations in the gap function and solve the resulting eigenvalue problem for T_c. We also extract isotope effect coefficients α from the relation

$$\alpha = \frac{1}{2}\left.\frac{d\ln T_c}{d\ln \Omega_0}\right|_\lambda \quad (4)$$

by changing the Einstein phonon frequency Ω_0 a small amount and adjusting g^2 so that $\lambda = 2g^2/\Omega_0 W$, W the bandwidth, is constant.

In order to complete the specification of the problem, we must discuss the band structures used to determine $N(E)$ and the choice of coupling constants. We obtain the electronic dispersion $E_{\mathbf{k}}$ by fitting to a two-dimensional, tight-binding form $E_{\mathbf{k}} = \sum_{i=0}^{5} t_i \eta_i(\mathbf{k})$ with the basis functions $\eta_i(\mathbf{k})$ listed in Table I and the parameters t_i in Table II. Representative dispersions for LSCO and BSCCO are shown in Fig. 1.

Our fitted band structures are obtained from different procedures, which we will now describe. For the LSCO case, a simple two-parameter fit was done to a LDA band-structure calculation with a 2 eV bandwidth. For the YBCO case, we perform three fits to the data. The first fit was done by assuming a 2 eV bandwidth as in LSCO and adding a third tight-binding term to force

TABLE I. Two-dimensional, tight-binding basis functions used in the fits of the energy dispersion described in the text in units of the lattice spacing (a square unit cell is assumed).

i	$\eta_i(\mathbf{k})$
0	1
1	$\frac{1}{2}(\cos k_x + \cos k_y)$
2	$\cos k_x \cos k_y$
3	$\frac{1}{2}(\cos 2k_x + \cos 2k_y)$
4	$\frac{1}{2}(\cos 2k_x \cos k_y + \cos k_x \cos 2k_y)$
5	$\cos 2k_x \cos 2k_y$

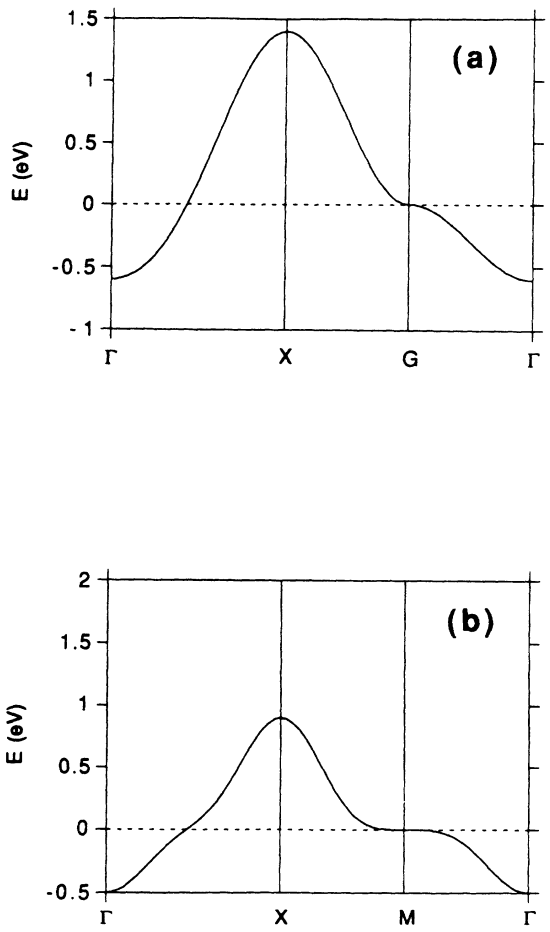

FIG. 1. Electronic energy dispersion along high-symmetry directions in the Brillouin zone resulting from fits of (a) a LDA band-structure calculation for LSCO and (b) ARPES measurements on BSCCO (Ref. 11) to the tight-binding form described in the text. The wave vectors in the two-dimensional Brillouin zone are $\Gamma = (0,0)$, $X = (\pi,\pi)$, and G (M) $= (\pi, 0)$.

TABLE II. Parameters t_i in eV corresponding to the basis functions in Table I used to fit the LDA calculations and photoemission measurements of several cuprate superconductors. When t_i is zero, this parameter was not included in the fit. For YBCO, in parenthesis are the bandwidth (eV) and saddle point type (ext for extended, bf for bifurcated).

	LSCO	YBCO(1,ext)	YBCO(2,ext)	YBCO(2,bf)	BSCCO
t_0	0.00	0.00	0.00	0.00	0.0607
t_1	-1.00	-0.50	-1.00	-1.00	-0.525
t_2	0.20	0.15	0.38	0.38	0.100
t_3	0.00	-0.05	-0.06	-0.09	0.0287
t_4	0.00	0.00	0.00	0.00	-0.175
t_5	0.00	0.00	0.00	0.00	0.0107

a k^4 dependence along the k_x direction around the $(\pi,0)$ point. This procedure gives an extended saddle point and so approximates the photoemission data.[9,10] A second fit was done by relaxing the third parameter to best fit all the data along $(0,0)$ to $(\pi,0)$. This fit splits the extended singularity at $(\pi,0)$ into two nearby logarithmic singularities (bifurcated saddle points) as seen in LDA calculations, which are related to the displacement of the planar oxygens along the c axis of the crystal.[20] [The data are more consistent with an extended saddle point about $(\pi,0)$ than with bifurcated saddle points. The flatness of the experimental bands is almost certainly a correlation effect, which can only be approximately simulated by the tight-binding fit.] The third fit assumed a 1 eV bandwidth and gives a better fit to the data along the $(\pi,0)$ to (π,π) direction, which are consistent with a quadratic dispersion about $(\pi,0)$; however, as this point is only 20 meV below the Fermi energy, little information is available before the band disperses through the Fermi energy. For BSCCO, the tight-binding fit was done to the proposed band structure presented by Dessau *et al.* based on their photoemission data and yields a bandwidth of 1.4 eV.[11] The dispersion was fit so as to go like k^4 along both orthogonal directions about the $(\pi,0)$ point. For comparison, we also include calculations for a flat density of states with a 2 eV bandwidth.

In computing the density of states from these energy dispersions, we employ a two-dimensional "tetrahedron" code that produces data on an energy grid of spacing 0.1 meV near the singularity. We have checked that our results are insensitive to this mesh density and have reproduced our earlier calculations on a logarithmically divergent density of states where the singularity is treated exactly.[19] We find that, for the LSCO and bifurcated YBCO cases, the density of states has a logarithmic singularity. For the extended YBCO case, on the other hand, the divergence goes like the inverse fourth root of the energy difference from the singularity, and the divergence in BSCCO goes as the inverse square root. We remark that the densities of states are similar in both YBCO cases, even though the divergences are different. We see that, by studying these different materials, we are actually studying different Van Hove singularity strengths.

The choice of coupling constant in our calculations is complicated due to the sharp structure in the density of states. In a material with a structureless density of states, the coupling strength is $\lambda = 2g^2/W\Omega_0$. However, the magnitude of the coupling extracted from transport measurements will be renormalized by singularities in the density of states, and so a more physical choice of coupling is to use the self-consistently calculated self-energy at the lowest Matsubara frequency $\omega_0 = \pi T_c$: $\lambda_Z = -\mathrm{Im}\,\Sigma(i\omega_0)/\omega_0$. In what follows, we will show calculations with either λ or λ_Z fixed and examine the differences.

For completeness, we will discuss some caveats regarding our approach. First, our calculations employ a mean field theory where vertex corrections are ignored. Although justified by Migdal's theorem[21] in conventional phonon-mediated superconductors with flat densities of states, this approximation may fail when the density of states is singular. Recent work has indicated that, for a logarithmic Van Hove singularity, vertex corrections may not be large and may actually reduce the computed T_c,[22] but the case of a power law singularity has not been examined. Second, it has been pointed out that, because the electronic density of states enters into the screening of the electron-phonon matrix element, ignoring the detailed wave vector dependence of this matrix element and the phonon propagator—as we do—could lead to erroneous results.[23,24] Third, phase-space restrictions on electron-electron scattering imposed by the Van Hove singularity enhances the electronic response functions, possibly leading to an electronic pairing mechanism.[25] Our calculations focus on a phononlike pairing boson and so do not address this issue. Fourth, for YBCO, we consider only the plane band which contains the Van Hove singularity nearest the Fermi energy (for BSCCO, the splitting of the two CuO plane bands is ignored). We expect that this band will dominate the properties of the material, but full multiband calculations will be required to test this assertion. We therefore view the results of this paper as a first step in identifying the quantitative effect of a singular density of states on T_c when strong-coupling effects are included and leave these other extensions for future work.

Having described our approach, we will now discuss our results, beginning with our weak-coupling calculations. For these computations, we drop the τ_0 and τ_3 components of the self-energy from the Eliashberg equations, and we fix λ to 0.211 in order to obtain a 95 K T_c for the YBCO band structure with the extended Van Hove singularity and 2 eV bandwidth. Note that this

weak-coupling calculation is not equivalent to the standard BCS calculation with a square well potential, but does serve to illustrate the effect of neglecting inelastic pair breaking.

The maximum T_c occurs at a band filling near but not necessarily at the Van Hove singularity, and we tabulate these maximum critical temperatures and isotope effect coefficients as a function of material type in Table III. We observe that the maximum weak-coupling T_c's are enhanced by factors of 17 (LSCO) to 45 (BSCCO) over the flat density of states value and that this enhancement follows the strength of the singularity, increasing as the divergence goes from logarithmic for LSCO to fourth root for the extended YBCO to square root for BSCCO. In contrast, the isotope effect coefficient decreases systematically with singularity strength from the BCS result of 0.50 for the flat density of states to 0.20 for BSCCO. We also see that the extended and bifurcated densities of states for YBCO yield approximately equal T_c's, despite the differences in singular behavior. Reducing the bandwidth by one-half, though, reduces T_c by 40%, despite working at fixed λ. The isotope effect coefficient, however, is unaffected by this change. Finally, note that the critical temperature roughly doubles from the logarithmically divergent LSCO model to the fourth-root divergent extended YBCO model, similar to the T_c's of the actual materials. This observation leads to the speculation that the pairing interaction is the same in LSCO and YBCO with the difference in critical temperatures accounted for solely by the band structure.

The strong-coupling calculations do not support this simple view, however. In Table III, we show strong-coupling results for the maximum T_c obtained from the solution of the Eliashberg equations including all components of the self-energy and with $\lambda = 0.627$, chosen once again in order to fix the T_c for the W = 2 eV extended YBCO band structure to 95 K. We see that the critical temperatures still show a systematic increase with the strength of the singularity, but the strong-coupling T_c's show less sensitivity to the singularity strength than the weak-coupling T_c's: the maximum strong-coupling T_c is enhanced by factors of only 2.6 (LSCO) to 3.4 (BSCCO) relative to the flat density of states T_c. Similarly, the strong-coupling isotope effect coefficient still exhibits a systematic decrease with singularity strength, but the magnitude of this trend is severely reduced, leaving α roughly constant at 0.4. We also note that the finite bandwidth and strong-coupling effects combine to increase the flat density of states α to 0.51 instead of 0.50. As with the weak-coupling calculations, the extended and bifurcated densities of states yield similar T_c's, α's, and λ_Z's; reducing the bandwidth to 1 eV reduces T_c and λ_Z by approximately 20% but leaves α almost unchanged.

Drawing these results together, we can say that, in both weak- and strong-coupling calculations, T_c and α show systematic trends with the strength of the divergence in the density of states, but the magnitude of this effect is reduced in the strong-coupling calculations. In particular, we find that the isotope effect coefficient in strong coupling is almost independent of the strength of the singularity and is around 0.4, which is much larger than the observed α's in the optimally doped cuprates. Also, the enhancement of T_c relative to the flat density of states in strong coupling is two to three for our choice of λ, as shown earlier for a logarithmically singular density of states.[19] Furthermore, we find that these results are robust against the parameterization of the YBCO data (extended vs bifurcated), but T_c and λ_Z are found to be sensitive to band width (although α is not).

Additionally, the idea of a universal pairing interaction does not seem to be supported by the strong-coupling calculations. By fixing the coupling in the extended parametrization of YBCO to give a strong-coupling T_c of 95 K, we find that the maximum T_c for LSCO becomes 78 K, much larger than the observed maximum T_c of 40 K. This result casts doubt on the idea that the differences in T_c are simply due to band-structure effects. We should also remark that the experimental T_c for BSCCO is lower than YBCO, despite the more singular density of states inferred for the former. We show a plot of T_c versus doping for this λ in Fig. 2, which illustrates in greater detail both the reduced difference in T_c and the enhancement of T_c over that given by a flat density of states.

There are several other features of Fig. 2 which should be pointed out. First, we note that the critical temperature rises around the Van Hove singularity, and the width of this maximum broadens as the strength of the singu-

TABLE III. Band filling corresponding to maximum critical temperature, $n_{\max}$, maximum critical temperature, $T_c^{\max}$, isotope effect coefficient, α, and self-consistent coupling constant, λ_Z, for the densities of states discussed in the text. Results are obtained from weak-coupling Eliashberg theory with $\lambda = 0.211$ and strong-coupling Eliashberg theory with $\lambda = 0.627$ in order to give a 95 K T_c in the extended YBCO band structure with 2 eV bandwidth. YBCO notation as in Table II.

	Flat	LSCO	YBCO(1,ext)	YBCO(2,ext)	YBCO(2,bf)	BSCCO
$n_{\max}$	1.00	0.82	0.55	0.48	0.45	0.92
Weak coupling						
$T_c^{\max}$ (K)	3.1	54.2	59.4	95.0	97.5	139
α	0.50	0.34	0.28	0.28	0.27	0.20
Strong coupling						
$T_c^{\max}$ (K)	30.5	78.0	77.9	95.0	94.9	105
α	0.51	0.43	0.40	0.41	0.41	0.40
λ_Z	0.59	1.07	0.96	1.30	1.29	1.45

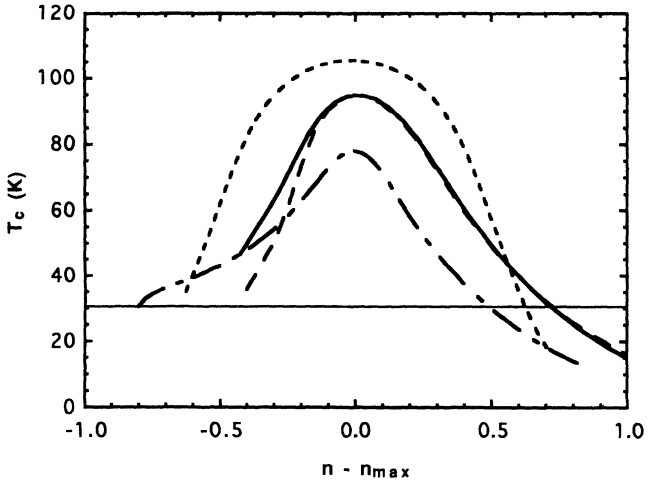

FIG. 2. Critical temperature T_c in K as a function of the number of electrons per unit cell away from the optimum value $n - n_{max}$ computed for the tight-binding band structures corresponding to BSCCO (short-dashed line), bifurcated YBCO (long-dashed line), extended YBCO with 2 eV bandwidth (solid line), and LSCO (dot-dashed line). The horizontal solid line is the value of T_c for the flat density of states at half-filling. These results are produced by strong-coupling Eliashberg theory with an Einstein phonon of energy Ω_0 = 500 K and λ = 0.627. See Table III for additional results at optimal doping n_{max}.

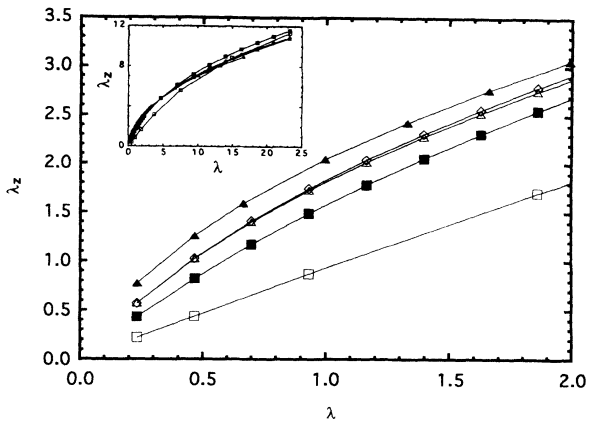

FIG. 3. Self-consistent coupling constant λ_Z as a function of the bare coupling constant λ for the band structures corresponding to LSCO (solid boxes), YBCO with the extended (open diamonds), and bifurcated (open triangles) Van Hove singularities and 2 eV bandwidths, BSCCO (solid triangles), and a flat density of states of 2 eV bandwidth (open boxes). The lines are to guide the eye. The λ_Z's result from the solution of the strong-coupling Eliashberg equations as described in the text. Inset: data from the main figure displayed out to large λ.

larity increases. Away from the singularity, the T_c falls below the flat density of states value. This behavior is a reflection of the redistribution of electronic states caused by the Van Hove singularity; basically, spectral weight is transferred from the band edge to the singularity, and T_c follows this shift. Second, at low values of n, the plotted data show somewhat more complicated behavior due to the effect of the band edge. Finally, we see that the extended and bifurcated YBCO give similar T_c versus doping curves despite the differing singular behavior. The density of states peak in the extended case is higher than the bifurcated case but is also narrower in energy. This result supports the idea that what determines T_c is an effective density of states which is a particular average of the actual density of states over the scale of the phonon energy Ω_0.[4,5]

In looking at the self-consistent coupling strength λ_Z in Table III, we see that λ_Z is larger than λ for the singular densities of states by a factor of order 2, implying that these calculations are in the strong-coupling regime. The systematic behavior of λ_Z with λ is shown in Fig. 3. For a flat density of states and an infinite bandwidth, λ_Z = λ. For the finite bandwidths used here, this relation is valid only in the limit of small λ. As seen in the inset to Fig. 3, at larger λ, the flat density of states λ_Z is less than λ by about a factor of 2. On the other hand, when the density of states is singular, λ_Z is enhanced at small λ, and the magnitude of the enhancement grows as λ decreases and as the strength of the singularity increases. This behavior arises from the availability of more scattering states near the Van Hove singularity. At large λ, however, the structure in the interacting density of states is smeared out by the strong scattering, and λ_Z for the singular density of states begins to behave more like that for a flat density of states; i.e., it is dominated by the finite bandwidth. The curves come together at large λ as shown in the inset to Fig. 3.

Since both T_c and λ_Z are enhanced by the Van Hove singularity, plotting the one quantity as a function of the other is instructive. To that end, we show in Fig. 4

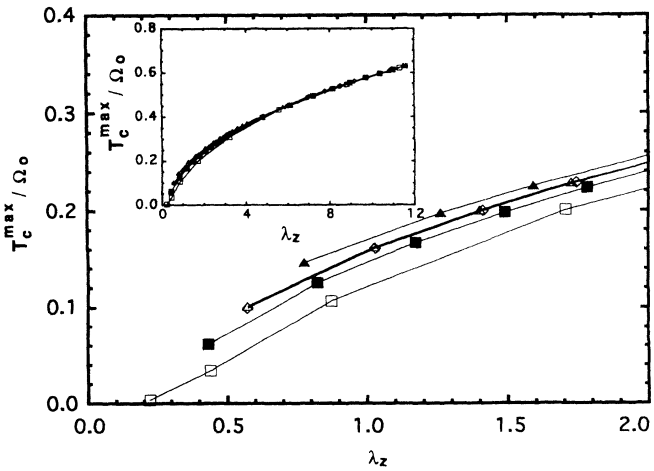

FIG. 4. Maximum critical temperature T_c^{max} normalized by the Einstein phonon frequency Ω_0 as a function of the self-consistently determined λ_Z. Symbols are the same as in Fig. 3, as is the method of computation. Inset: data from the main figure displayed out to large λ_Z in order to demonstrate the absence of density of states effects at very strong coupling.

the maximum transition temperature T_c^{max} normalized by the Einstein phonon frequency Ω_0 plotted against the self-consistent λ_Z for all the materials studied and with the results for a flat density of states included for comparison. Our results for the flat density of states reproduce the standard curve at small λ_Z.[26] Also at small λ_Z, T_c is still strongly and systematically enhanced by an increasingly singular density of states compared to the results for the structureless density of states. This enhancement is reduced at stronger coupling, becoming at most around 50% for $\lambda_Z \approx 1$. At still stronger coupling, as seen in the inset to Fig. 4, the effect of the singularity in the density of states is completely removed and the critical temperature follows the results for a structureless density of states. If T_c^{max}/Ω_0 is plotted against the bare λ, the qualitative features of the curve are the same, but the T_c enhancement is larger as one would expect from Table III and the results at very strong coupling do not scale as well as when the T_c's are plotted against λ_Z.

We can understand these results in the following way. At small λ, λ_Z is strongly enhanced by the presence of a singularity in the density of states, but it is approximately equal to λ if there is no such structure. Comparison of critical temperatures at fixed λ_Z therefore means that a much larger value of λ is used in the flat density of states calculation and so the apparent effect of the singular density of states is reduced. At strong coupling, the enhanced scattering from the singular bare density of states acts to smear out the interacting density of states and so there is no T_c enhancement. We note that the loss of the Van Hove singularity in the interacting density of states at strong coupling has been seen explicitly in recent calculations.[16,17]

It is clear from our results that strong-coupling calculations are required to make physical predictions of the critical temperature. The remaining question is: should one compare these strong-coupling critical temperatures at fixed λ or fixed λ_Z? In our investigation of the possibility of a universal pairing interaction, it is the microscopic coupling g and phonon energy Ω_0 which would be fixed, yielding—for a given bandwidth—a fixed λ. Our results in this case show little evidence for a universal pairing interaction due to the reduction of the effect of the Van Hove singularity on T_c. Alternatively, one can extract an effective coupling constant from transport measurements which would include the self-consistent effects of the density of states and so could be used to fix λ_Z. From earlier work,[27,19] we found that the canonical values of $\lambda_{tr} \approx 0.2$–0.4 extracted from optical conductivity measurements in YBCO correspond to $\lambda_Z \approx 1$, at least if spin fluctuations are the source of the resistivity. Similar estimates of λ_Z have appeared in the literature regarding phonon coupling strengths.[28] Based on this result and Fig. 4, we conclude that, while the Van Hove singularity does enhance T_c systematically with the strength of the divergence in the density of states, the enhancement factor in this parameter region is at most around 50% and so by itself cannot account for the large T_c's observed. In order to obtain a large T_c, either a large pairing interaction energy Ω_0 or a modification of the pairing interaction due to the singularity is required, but it is not known whether either effect is consistent with the observed linear resistivity of the cuprates.

In conclusion, we have performed Eliashberg computations of the critical temperature in superconductors with strongly singular densities of states chosen to model LSCO, YBCO, and BSCCO. We have demonstrated that, while the weak-coupling solutions do suggest a strong influence of the strength of the Van Hove singularity on T_c and the existence of a universal pairing interaction in the cuprates, strong-coupling calculations show a reduced sensitivity to the singularity strength and do not support the notion that band-structure effects alone can account for either the large T_c's or the different T_c's within the family of copper oxide superconductors. The reduced effect of the Van Hove singularities can be traced to the fact that the inelastic scattering included in strong-coupling calculations smears out the sharp structure in the density of states, producing a T_c similar to that from a flat density of states. This effect is seen clearly when the results are plotted as a function of the physically relevant self-consistent coupling constant λ_Z and leads to universal behavior at very strong coupling. If the Van Hove singularities in the electronic band structures of the cuprates are responsible for high-temperature superconductivity, then the effect must come in through vertex corrections, screening effects in the electron-pairing boson matrix elements, direct electronic interactions, or multiband effects. Based on the results of this work, investigation into these effects now acquires additional importance.

The authors would like to thank J. C. Campuzano and K. Gofron for making their YBCO photoemission data available to us and A. A. Abrikosov for copies of his unpublished papers. This work was supported by the National Science Foundation (DMR 91-20000) through the Science and Technology Center for Superconductivity and DMR-MRL-8819860 (R.J.R.) and by the U.S. Department of Energy, Basic Energy Sciences, under Contract No. W-31-109-ENG-38 (M.R.N.).

* Present address: Department of Physics, University of Maryland, College Park, MD 20742.

[1] J. Labbé, S. Barišić, and J. Friedel, Phys. Rev. Lett. **19**, 1039 (1967); S. Barišić, Phys. Rev. B **5**, 932 (1972).

[2] S. G. Lie and J. P. Carbotte, Solid State Commun. **34**, 599 (1980).

[3] P. Horsch and H. Rietschel, Z. Phys. B **27**, 153 (1977); S. J. Nettel and H. Thomas, Solid State Commun. **21**, 683 (1977).

[4] B. Mitrović and J. P. Carbotte, Solid State Commun. **40**, 249 (1981); Can. J. Phys. **61**, 758 (1983); **61**, 784 (1983). See also S. G. Lie and J. P. Carbotte, Solid State Commun. **26**, 511 (1978); **35**, 127 (1980); E. Schachinger, B. Mitrović, and J. P. Carbotte, J. Phys. F **12**, 1771 (1982); E. Schachinger, M. G. Greeson, and J. P. Carbotte, Phys. Rev. B **42**, 406 (1990).

[5] W. E. Pickett, Phys. Rev. B **21**, 3897 (1980); **26**, 1186 (1982); W. E. Pickett and B. M. Klein, Solid State Commun. **38**, 95 (1981).
[6] R. Combescot and J. Labbé, Physica C **153-155**, 204 (1988); J. Friedel, J. Phys.: Condens. Matter. **1**, 7757 (1989).
[7] D. M. Newns, C. C. Tsuei, P. C. Pattnaik, and C. L. Kane, Comments Condens. Matter Phys. **15**, 273 (1992); C. C. Tsuei, D. M. Newns, C. C. Chi, and P. C. Pattnaik, Phys. Rev. Lett. **65**, 2724 (1990); C. C. Tsuei, D. M. Newns, C. C. Chi, P. C. Pattnaik, and M. Däumling, *ibid.* **69**, 2134 (1992).
[8] R. S. Markiewicz, Int. J. Mod. Phys. B **5**, 2037 (1991); Physica C **217**, 381 (1993).
[9] K. Gofron, J. C. Campuzano, H. Ding, C. Gu, R. Liu, B. Dabrowski, B. W. Veal, W. Cramer, and G. Jennings, J. Phys. Chem. Solids **54**, 1193 (1993); (unpublished).
[10] A. A. Abrikosov, J. C. Campuzano, and K. Gofron, Physica C **214**, 73 (1993).
[11] D. S. Dessau, Z.-X. Shen, D. M. King, D. S. Marshall, L. W. Lombardo, P. H. Dickinson, A. G. Loeser, J. DiCarlo, C.-H. Park, A. Kapitulnik, and W. E. Spicer, Phys. Rev. Lett. **71**, 2781 (1993).
[12] J. E. Hirsch and D. J. Scalapino, Phys. Rev. Lett. **56**, 2732 (1986).
[13] R. S. Markiewicz, Physica C **183**, 303 (1991).
[14] R. Combescot, Phys. Rev. Lett. **68**, 1089 (1992).
[15] S. Takács, Phys. Rev. B **48**, 13 127 (1993).
[16] D. R. Penn and M. L. Cohen, Phys. Rev. B **46**, 5466 (1992).
[17] J. Zhong and H.-B. Schüttler (unpublished).
[18] See, for example, P. B. Allen and B. Mitrović, in *Solid State Physics*, edited by H. Ehrenreich, F. Seitz, and D. Turnbull (Academic, New York, 1982), Vol. 37.
[19] R. J. Radtke, K. Levin, H.-B. Schüttler, and M. R. Norman, Phys. Rev. B **48**, 15 957 (1993).
[20] O. K. Andersen, A. I. Liechtenstein, C. O. Rodriguez, I. I. Mazin, O. Jepsen, V. P. Antropov, O. Gunnarsson, and S. Gopalan, Physica C **185-189**, 147 (1991); O. K. Andersen, O. Jepsen, A. I. Liechtenstein, and I. I. Mazin, Phys. Rev. B **49**, 4145 (1994).
[21] A. B. Migdal, Zh. Eksp. Teor. Fiz. **34**, 1438 (1961) [Sov. Phys. JETP **7**, 996 (1958)].
[22] H. R. Krishnamurthy, D. M. Newns, P. C. Pattnaik, C. C. Tsuei, and C. C. Chi, Phys. Rev. B **49**, 3520 (1994).
[23] G. D. Mahan, Phys. Rev. B **48**, 16 557 (1993).
[24] A. A. Abrikosov, Physica C **222**, 191 (1994).
[25] D. M. Newns, H. R. Krishnamurthy, P. C. Pattnaik, C. C. Tsuei, and C. L. Kane, Phys. Rev. Lett. **69**, 1264 (1992).
[26] P. B. Allen and R. C. Dynes, Phys. Rev. B **12**, 905 (1975).
[27] R. J. Radtke, S. Ullah, K. Levin, and M. R. Norman, Phys. Rev. B **46**, 11 975 (1992).
[28] P. B. Allen, Comments Condens. Matter. Phys. **15**, 327 (1992).